

Environmental Science Advances

Accepted Manuscript

This article can be cited before page numbers have been issued, to do this please use: G. Bhardwaj, L. Wankhede, R. Kumar Das, A. Eldyasti, A. Koubaa and S. Kaur Brar, *Environ. Sci.: Adv.*, 2026, DOI: 10.1039/D6VA00023A.



This is an Accepted Manuscript, which has been through the Royal Society of Chemistry peer review process and has been accepted for publication.

Accepted Manuscripts are published online shortly after acceptance, before technical editing, formatting and proof reading. Using this free service, authors can make their results available to the community, in citable form, before we publish the edited article. We will replace this Accepted Manuscript with the edited and formatted Advance Article as soon as it is available.

You can find more information about Accepted Manuscripts in the [Information for Authors](#).

Please note that technical editing may introduce minor changes to the text and/or graphics, which may alter content. The journal's standard [Terms & Conditions](#) and the [Ethical guidelines](#) still apply. In no event shall the Royal Society of Chemistry be held responsible for any errors or omissions in this Accepted Manuscript or any consequences arising from the use of any information it contains.

Environmental Significance Statement

View Article Online
DOI: 10.1039/D6VA00023A

Microplastics are pervasive in wastewater treatment plants, where they interact with microbial communities and influence the dynamics of contaminants and pathogens. While their impacts on treatment performance have been widely reported, the underlying mechanisms governing microplastic–microbe interactions remain poorly understood. This knowledge gap limits our ability to accurately assess microplastics fate, associated risks, and potential mitigation strategies in engineered water systems. This study demonstrates that biofilm formation on microplastics is polymer-specific, with biodegradable plastics selectively enriching plastic-degrading microorganisms, while certain conventional plastics preferentially accumulate opportunistic pathogens. These findings reveal biofilm-mediated pathways through which microplastics are transformed and biologically partitioned in wastewater treatment, with important implications for microplastic persistence, pathogen retention in sludge, and downstream environmental exposure.



1 **Deciphering the plastisphere nexus in biological wastewater treatment: distinct** View Article Online
DOI: 10.1039/D6VA00023A
2 **microbial colonization on biodegradable and conventional microplastics**

3 Gaurav Bhardwaj¹, Lachi Wankhede¹, Ratul Kumar Das¹, Ahmed Eldyasti¹, Ahmed Koubaa²,
4 Satinder Kaur Brar^{1*}

5 ¹Civil Engineering Department, Lassonde School of Engineering, York University, North
6 York, Ontario M3J1P3, Canada.

7 ²Forest Research Institute (Institut de recherche sur les forêts–IRF), Université du Québec en
8 Abitibi–Témiscamingue (UQAT), 445 Boul. de l'Université, Rouyn-Noranda J9X 5E4, QC,
9 Canada

10 *Corresponding author: Satinder Kaur Brar (satinder.brar@lassonde.yorku.ca)

11 **Abstract**

12 Microplastics (MPs) are ubiquitous in wastewater treatment plants (WWTPs), where their
13 persistent presence has been shown to alter treatment performance and microbial community
14 structure. However, existing studies largely emphasize bulk system responses, while the
15 underlying mechanisms, including biofilm formation on MP surfaces, remain insufficiently
16 characterized. In particular, the extent to which microbial colonization on MP surfaces is
17 selective, polymer-dependent and evolves over time under WWTP conditions remains poorly
18 resolved. To address this gap, this study systematically compares plastisphere development on
19 four conventional polymers, polyethylene (PE), polypropylene (PP), polystyrene (PS), and
20 polyethylene terephthalate (PET), and a biodegradable polymer, polylactic acid (PLA) under
21 sequencing batch reactor (SBR) conditions. Biofilm biomass increased up to 5-fold, with PLA
22 exhibiting the highest accumulation ($OD_{595nm} = 1.067$; $p < 0.05$), substantially exceeding
23 conventional MPs. Intrinsic polymer properties shaped microbial colonization through
24 selective enrichment on MP surfaces. While PLA supported a transient peak in community
25 diversity and selectively enriched plastic-degrading taxa such as *Comamonas* (~16–25%),



26 continuous hydrolytic oxidation and surface pitting prevented stable long-term community
27 retention. In contrast, conventional MPs converged toward low-diversity biofilms dominated
28 by pioneer genera including *Raoultella* (~80–90%). Among conventional MPs, PS exhibited
29 the strongest divergence at biofilm maturity, functioning as a persistent reservoir for ESKAPE
30 pathogens. PS specifically enriched *Acinetobacter* (8.17 log₂-fold-change), demonstrating that
31 while biodegradable surfaces promote robust general microbial growth, the structural
32 permanence of conventional microplastics provides a more selective and reliable substrate for
33 long-term pathogen persistence. Together, these findings highlight polymer-specific
34 plastisphere development as a key biological pathway governing MP transformation and
35 microbial partitioning in WWTPs, with implications for MP fate and sludge-associated
36 microbial risks.

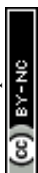
37 1. Introduction

38 Microplastics (MPs) are plastic particles smaller than 5 mm that arise as primary pellets or as
39 secondary fragments from the degradation of larger plastic debris¹. MPs are a global concern,
40 particularly due to their presence and persistence in aquatic environments². In these settings,
41 microbes rapidly colonize MP surfaces and form the plastisphere, a structured biofilm
42 embedded in extracellular polymeric substances (EPS)³. The EPS matrix supports adhesion,
43 protection from stressors, and cell-cell communication through quorum signalling⁴. MP-
44 associated biofilms can enrich opportunistic pathogens and antibiotic resistance genes (ARGs),
45 while EPS can promote horizontal gene transfer (HGT) by concentrating extracellular DNA
46 and bringing cells into close contact^{5,6}. The small size, low density, and hydrophobicity of MPs
47 favour long-range transport and persistence, which may amplify the spread of pathogens and
48 ARGs with implications for ecosystems and human health^{7,8}.

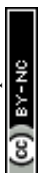


49 Biofilm formation on MPs proceeds through distinct stages: initial colonization, reversible
50 adhesion transitioning to irreversible attachment, growth, and dispersion⁹. MP properties and
51 environmental conditions govern these dynamics alongside exposure duration^{10,11}.
52 Hydrophobicity and surface energy guide the initial adhesion, while roughness, charge, and
53 weathering-driven oxidation stabilize the EPS matrix¹². Concurrent gradients in nutrients,
54 oxygen, and shear drive succession from early colonizers to mature consortia¹³. Co-occurring
55 stressors, such as antibiotics, metals, and organic micropollutants, also impose selection that
56 further structures the plastsphere¹⁴.

57 Previous plastsphere research has largely centred on freshwater and marine systems^{15,16}, while
58 wastewater treatment plants (WWTPs) are comparatively overlooked despite acting as major
59 conduits to receiving waters, with individual facilities discharging up to 5×10^7 MPs day⁻¹¹⁷.
60 This effluent load represents roughly the residual 1 % of incoming MPs; the remaining 99 %
61 are retained and partitioned to sewage sludge, where 1,500–170,000 MPs kg⁻¹ dry weight have
62 been reported¹⁸. This accumulation is significant because MPs interact with microorganisms
63 and can release or carry toxic compounds, which may affect biological treatment processes.
64 Consequently, most MP studies in WWTPs have emphasized treatment efficiency and sludge
65 microbiology^{19,20}. Yet this focus often overlooks the underlying mechanism in biological
66 wastewater treatment units, the biofilm formation on MP surfaces. The dense microbial
67 consortia, continuous substrate supply, controlled hydrodynamics, and strong nutrient and
68 oxygen gradients within these treatment units collectively create near-optimal conditions
69 favouring biofilm formation on MPs. This underrepresentation constitutes a prominent
70 research gap: understanding the plastsphere within biological treatment units of WWTPs.
71 Closing this knowledge gap is essential for understanding how the biological processes in
72 WWTPs influence the selection of microorganisms specific to MPs, pathogen enrichment, and
73 MP weathering processes.



74 Previous studies of the wastewater plastisphere have shown that MP-attached microbial
75 communities differ from those in bulk sludge, forming a distinct plastisphere²¹. However, the
76 extent to which this plastisphere varies by polymer type remains largely unexplored in
77 WWTPs. Feng et al. (2023) compared polyethylene terephthalate (PET), polystyrene (PS),
78 polycarbonate (PC), and polyethylene (PE) in the aerobic and anaerobic tanks of a WWTP, but
79 did not include any biodegradable plastics²². Although biodegradable polymers such as
80 polylactic acid (PLA) accumulate in WWTPs and often exhibit higher adsorption affinity and
81 act as stronger microbial and chemical carriers than non-biodegradable MPs²³, direct
82 comparisons between biodegradable and non-biodegradable MPs remain scarce. A few
83 comparisons of conventional versus biodegradable MPs exist; for instance, Martínez-Campos
84 et al. evaluated four conventional and three biodegradable polymers but focused only on the
85 first 48 hours of colonization, leaving later stages and succession unaddressed²⁴. A direct
86 comparison of biofilm formation on conventional versus biodegradable MPs within wastewater
87 biological treatment units remains understudied across both early and long-term colonization.
88 To the best of our knowledge, it will be the first comprehensive reporting on the side-by-side
89 plastisphere comparison of five distinct MP polymers, four conventional (PE, PP, PS, PET)
90 and one biodegradable (PLA), in sequencing batch reactors (SBRs) over 30 days, resolving
91 both early and long-term colonization across defined biofilm stages. By using environmentally
92 relevant MP concentrations and identical test conditions for all MPs, this work overcomes the
93 inconsistency and limited comparability of previous studies. Accordingly, the objectives focus
94 on three main parts. The first objective is to quantify and compare differential biofilm
95 formation on conventional versus biodegradable MPs using identical SBRs over time. The
96 characterization of bacterial diversity and community structure of MP-attached consortia
97 across biofilm stages using 16S rRNA gene amplicon sequencing has been studied and
98 presented as the second objective of the study. The final objective is to systematically evaluate



99 the colonization and enrichment of pathogenic bacteria together with evidence for microbial
100 degradation and associated physicochemical weathering of MPs in WWTPs.

101 **2. Materials and Methods**

102 **2.1. Microplastics, experimental setup, and operation**

103 Five model MPs with distinct physicochemical properties and environmental relevance were
104 selected, including PLA (Ingeo™ 2003D, NatureWorks), PET (Arnite® A06700, DSM), PS
105 (STYRON 6860, Dow), PP (HG455FB, Borealis), and PE (Purell GA7760, LyondellBasell),
106 and were used in pellet form with the largest dimension of 3–4 mm. Before use, pellets were
107 rinsed with distilled water, sterilized in 70% ethanol for 30 min, rinsed with sterile phosphate-
108 buffered saline (PBS), and stored in sterile containers at room temperature. During start-up,
109 200 MPs were added per reactor, corresponding to 100 MPs g⁻¹ VSS, as a single dose under
110 aseptic conditions to ensure uniform exposure while limiting aggregation.

111 Reactor configuration and operational conditions followed an established SBR protocol
112 described previously²⁵. Briefly, eighteen identical cylindrical glass SBRs (1 L total volume;
113 0.40 L working volume; inner diameter 10.0 cm; total height 18 cm) were set up to run six
114 conditions in triplicate, five receiving a single MP type and one serving as an MP-free control.
115 Reactors were maintained at an ambient temperature of 25 ± 1 °C with orbital mixing at 180
116 rpm on 12 h cycles comprising 6 h aerobic and 4 h anoxic phases, with the remaining time
117 allocated to fill, settle, and decant. Synthetic wastewater was fed at the start of each cycle
118 (Supporting Information, Text S1), and 0.20 L was decanted at the end, yielding a hydraulic
119 retention time of 24 h.

120 **2.2. Analytical methods**

121 **2.2.1. Sampling design**



122 Sampling was conducted on days 3, 15, and 30 per reactor replicate. These time points
123 correspond to early colonization and transition to irreversible attachment (day 3),
124 growth and maturation (day 15), and late maturation with initial dispersion (day 30). A
125 30-day incubation represents 3-fold of the steady-state profile, and it is sufficient for
126 robust biofilm formation on MPs, consistent with prior studies²⁶.

127 At each time point, fifty MPs were aseptically removed per reactor for analysis. Low-
128 density MPs (PE and PP) floating on the surface were directly picked using sterile
129 forceps, while denser MPs (PS, PET, and PLA) were scooped from the reactor bottom
130 and then retrieved with forceps. The remaining MPs were left *in situ* for continued
131 exposure. Sludge samples (2 ml) were collected concurrently from the MP-free control
132 reactor to characterize the suspended microbial community.

133 2.2.2. Biofilm assessment

134 2.2.2.1. **Crystal violet assay:** Biofilm biomass on MPs was quantified by crystal
135 violet staining²⁷. Ten MPs per sample were rinsed three times with sterile
136 water to remove loosely attached cells and air-dried for 45 min at room
137 temperature. MPs were stained with 1% (w/v) crystal violet for 45 min,
138 washed three times with sterile water, and air-dried for 45 min. Bound dye
139 was solubilized in 1.0 mL of 95% (v/v) ethanol for 15 min, and the eluate
140 was transferred to a 96-well plate. Absorbance at 595 nm was measured
141 using a Synergy HT microplate reader (BioTek, Vermont, USA) with Gen5
142 software.

143 2.2.2.2. **Scanning electron microscopy (SEM):** Biofilm morphology on MPs
144 was characterized by SEM (Tescan VEGA). Samples were rinsed with 0.1
145 M PBS and fixed in 2.5% glutaraldehyde for 12 h at 4 °C. Fixed samples
146 were dehydrated through graded cold ethanol solutions (30, 50, 70, 90, and



147 100% v/v; 10 min each), mounted on aluminium stubs with carbon tape
148 sputter-coated with platinum using a Desktop V thin film deposition system,
149 and imaged at different magnification.

View Article Online
DOI: 10.1039/D6VA00023A

150 **2.2.3. DNA extraction and bacterial community analysis**

151 Genomic DNA was extracted from detached MP biofilms using the DNA Kit (GenBio
152 Systems, Inc., Canada) following the manufacturer's protocol. Yields from individual
153 replicates were insufficient for library preparation. Therefore, DNA from the three
154 reactor replicates per polymer per time point was pooled in equal mass before
155 sequencing. DNA purity and concentration were then assessed with a NanoDrop Lite
156 spectrophotometer (Thermo Scientific, USA). The V4 hypervariable region of the 16S
157 rRNA gene was amplified by PCR using the primer pair 515F
158 (GTGCCAGCMGCCGCGGTAA) and 806R (GGACTACNVGGGTWTCTAAT).
159 Subsequent library preparation, purification, and amplicon sequencing on an Illumina
160 platform were performed at the McMaster Genomics Facility, Faculty of Health
161 Sciences, McMaster University, Hamilton, Ontario, Canada. Raw reads were processed
162 with DADA2 package within the R software environment for quality filtering, error
163 correction, dereplication, paired-read merging, chimera removal, and inference of
164 amplicon sequence variants for downstream community analysis²⁸.

165 **2.2.4. Microplastic Characterization**

166 Surface morphology after 30 days of incubation was examined by SEM (Tescan
167 VEGA). Pristine MPs served as controls. Representative particles were mounted on
168 aluminum stubs with carbon tape, sputter-coated with platinum, and imaged at various
169 magnifications. Attenuated Total Reflectance - Fourier Transform Infrared (ATR-
170 FTIR) spectra were collected on a Bruker Alpha-P over 400–4000 cm⁻¹ with 16 scans



171 at 4 cm⁻¹ resolution for pristine and 30-day exposed MPs to assess changes in functional
172 groups. View Article Online
DOI: 10.1039/D6VA00023A

173 **2.2.5. Statistical analysis**

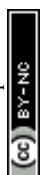
174 All statistical analyses and visualizations were performed in OriginPro 2025
175 (OriginLab, Northampton, USA). Differences in biofilm biomass across MP type and
176 time were tested by two-way repeated-measures analysis of variance (ANOVA),
177 followed by Tukey's post hoc comparisons; $p < 0.05$ was considered significant.
178 Microbial community analyses were conducted in Microbiome Analyst (version 2.0)²⁹.
179 To compare bacterial community compositions on different MP surfaces and assess the
180 factors influencing these communities, Alpha diversity was computed using Chao1,
181 Shannon, and Simpson indices. Beta diversity was assessed using Bray–Curtis
182 dissimilarities and visualized by principal coordinates analysis (PCoA).

183 **3. Results and discussion**

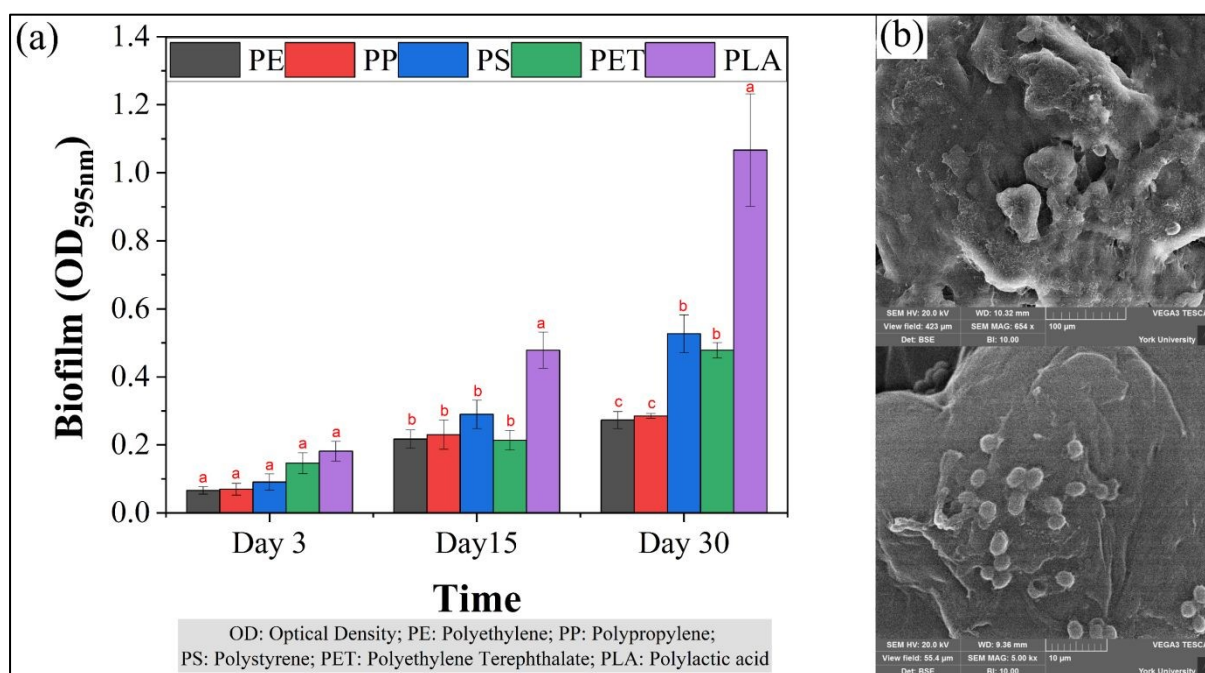
184 **3.1. Temporal dynamics of microplastic-associated biofilm**

185 Figure 1 (a) shows microbial biomass attached to MPs at days 3, 15, and 30, with a
186 representative SEM image of PLA at day 30 in Figure 1 (b). Across time, attached biomass
187 increased significantly from day 3, day 15 to day 30 for all polymers by two-way repeated-
188 measures ANOVA ($p < 0.05$). Over 30 days, biofilm levels rose by approximately 3 to 6-fold
189 across polymers, with PLA showing the steepest trajectory. These temporal patterns were
190 consistent with previous reports of significant biomass increases over 30-day incubations in
191 wastewater matrices³⁰.

192 Day 3 represented early colonization, with measurable but statistically indistinguishable
193 biomass across polymers as shown in Figure 1 (a). Biomass values ranged from approximately



194 0.07 to 0.18, with PLA highest at 0.182 ± 0.029 . These small differences aligned with the
 195 reversible-to-irreversible transition, during which conditioning films dominated adhesion.



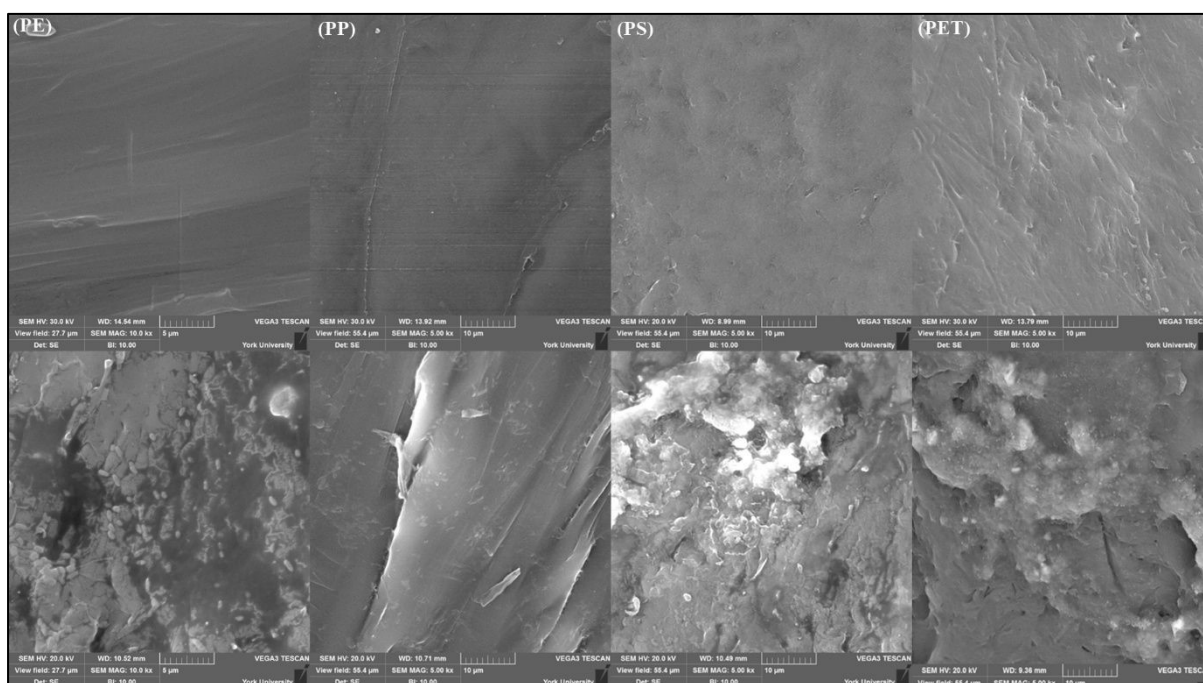
196
 197 Figure 1. (a) Temporal dynamics of biofilm formation on polyethylene (PE), polypropylene
 198 (PP), polystyrene (PS), polyethylene terephthalate (PET), and polylactic acid (PLA) MPs at
 199 days 3, 15, and 30. Bars represent mean \pm SD from triplicate reactors. Different letters above
 200 bars within the same time point indicate significant differences among polymer types based
 201 on two-way repeated-measures ANOVA followed by post hoc testing ($p < 0.05$). (b)
 202 Representative SEM micrograph of PLA at day 30 showing coccus microcolonies embedded
 203 in the EPS matrix.

204 By day 15, representing the growth and maturation stage, biomass had increased on all
 205 polymers (Figure 1 (a)). PLA showed significantly higher biofilm than the other MPs, reaching
 206 an OD of 0.478 ± 0.053 , approximately 1.6–2.2 times greater than that of the conventional
 207 polymers. Among the conventional polymers, PS (0.290 ± 0.041) was numerically higher than
 208 PET (0.213 ± 0.029), although this difference was not significant. This trend aligned with Feng
 209 et al., who observed more pronounced increases in PS surface roughness than in PET after 15-

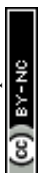


210 day incubation in aerobic reactors²². Taken together, the day 15 hierarchy likely reflected
 211 surface-governed processes. PLA underwent hydrolytic and oxidative modification that
 212 increased surface polarity and micro-roughness, which enhanced EPS anchoring. PS and PET
 213 showed intermediate accumulation because of their higher surface energies; PET also presented
 214 a polar, oxidizable surface. In contrast, the low-surface-energy polyolefins remained the least
 215 colonized.

216 By day 30, attached biomass had increased further for all polymers and resolved into three
 217 distinct tiers in Figure 1 (a): PLA was highest, PS and PET were intermediate, and PE and PP
 218 were lowest. PLA reached an OD of 1.067 ± 0.165 , approximately twice that of PS and PET
 219 and nearly four times that of PE and PP. The PLA micrograph revealed coccus microcolonies
 220 embedded within a dense EPS matrix, highlighting extensive biofilm accumulation on PLA
 221 (Figure 1 (b)). Representative SEM images detailing the distinct biofilm morphologies for the
 222 other MPs are shown in Figure 2.



223
 224 Figure 2. Representative SEM images MP-associated biofilms before and after 30-day
 225 incubation in SBRs.



226 The intermediate responses of PS and PET were consistent with their surface characteristics.
227 PS is an aromatic polymer with relatively high surface energy that promotes adhesion, and PET
228 is a polar, oxidizable polyester that supports EPS retention. Both outperformed the low-surface-
229 energy polyolefins under identical conditions but remained below PLA. These outcomes
230 aligned with prior evidence that biodegradable polymers aged more rapidly. Wang et al. (2025)
231 reported larger 30-day increases in FTIR carbonyl index for PLA than for PE and PET,
232 indicating greater oxidative weathering of biodegradable MPs, which increases surface polarity
233 and micro-roughness and helps explain the highest biomass observed on PLA³⁰.

234 Biofilm formation on MPs in SBRs followed the expected colonization stages: attachment,
235 growth, and maturation, with biomass steadily increasing over 30 days. Polymer type strongly
236 influenced these dynamics: biodegradable PLA fostered more robust colonization than
237 conventional polyolefins and polyesters. These insights are crucial for understanding the fate
238 of MPs in WWTPs and for optimizing treatment processes to mitigate their environmental
239 impact.

240 **3.2. Bacterial community ecology of MP-associated biofilms**

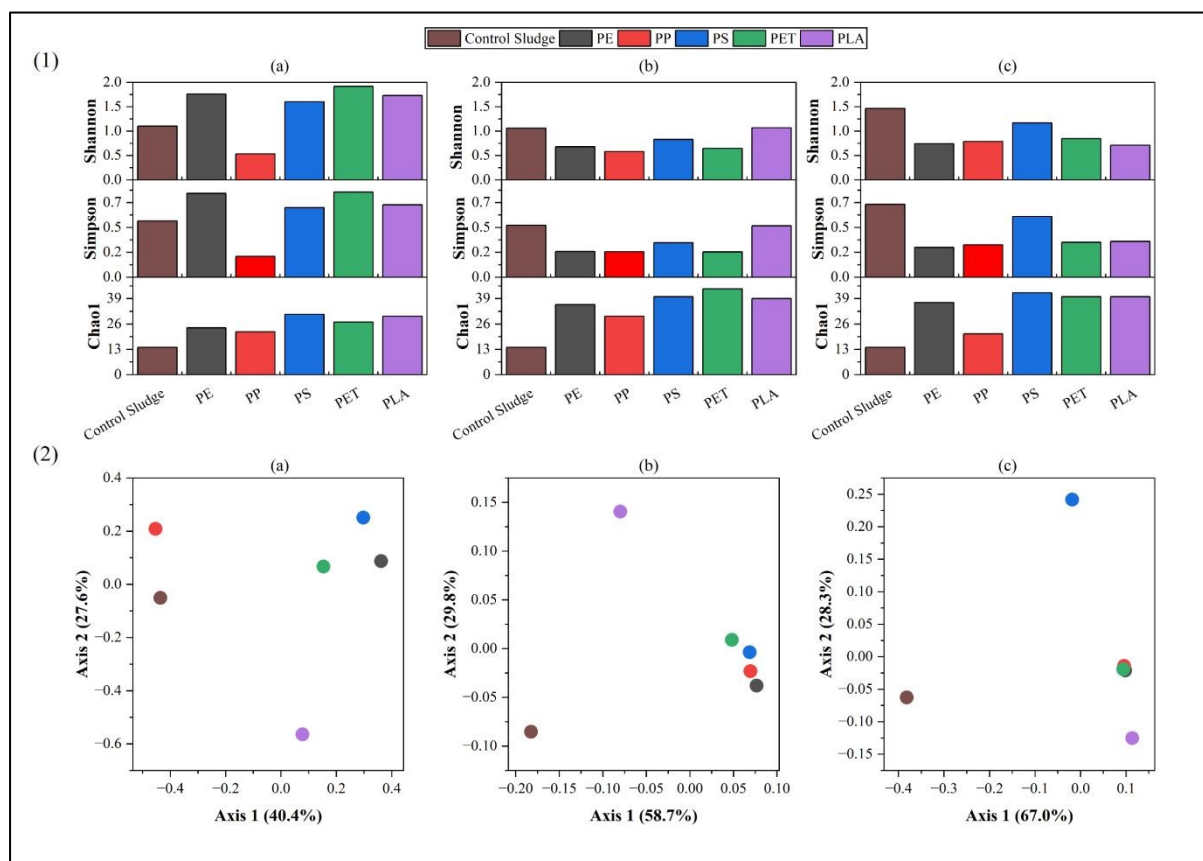
241 **3.2.1. Bacterial diversity**

242 16S rRNA gene amplicon sequencing profiled bacterial communities on MPs after 3, 15, and
243 30 days of incubation in SBRs. A total of 1,842,646 reads were obtained from 15 pooled
244 libraries (5 polymers × 3 sampling days). Alpha diversity, quantifying within-sample diversity,
245 and Beta diversity, capturing between-sample differences, were assessed as shown in Figure 3.

246 Alpha diversity was evaluated using Chao1 (richness), Simpson (evenness), and Shannon
247 (richness and evenness) indices (Figure 3 (1)). The control sludge exhibited a distinct diversity
248 profile compared to the MP-associated biofilms. Throughout the study, it maintained a



249 consistently lower species richness (Chao1). However, its overall diversity (Shannon and
 250 Simpson indices) remained relatively stable. Consequently, by day 30, the control sludge
 251 surpassed most MP communities in overall diversity as the plastispheres matured and
 252 specialized. This disparity highlighted the intense selective enrichment occurring on MP
 253 surfaces.



254
 255 Figure 3. Bacterial community diversity in microplastic-associated biofilms and sludge across
 256 time. (1) Alpha diversity for control, PE, PP, PS, PET, and PLA at: (a) day 3, (b) day 15, and
 257 (c) day 30 is shown as bar graphs for Shannon, Simpson, and Chao1. (2) Beta diversity by
 258 PCoA of Bray–Curtis dissimilarities at (a) day 3, (b) day 15, and (c) day 30.

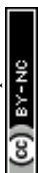
259 Across polymers, overall diversity and evenness, represented by the Shannon and Simpson
 260 indices, were highest at day 3, declined at day 15, and partially recovered by day 30.
 261 Conversely, species richness measured by the Chao1 index generally increased from day 3 to



262 day 15 across most MPs, indicating an accumulation of rare taxa as the biofilms developed.
263 Taken together, the indices indicated relatively even communities during early colonization
264 followed by a mid-stage consolidation. This consolidation was driven by dominance of a few
265 surface-adapted taxa that lowered overall evenness despite the concurrent increase in species
266 richness. A later re-balancing occurred as the communities mature. This temporal sequence
267 was consistent with prior work; for example, Lai et al. (2022) observed a diversity peak around
268 day 6, followed by a decline by day 16 during maturation³¹.

269 Polymer type governed the internal diversity dynamics within the MP-associated biofilms
270 (Figure 3(1)). For the biodegradable polymer PLA, within-sample diversity peaked at day 15,
271 where it supported the highest diversity among all MPs, before experiencing a sharp decline
272 by day 30. This temporal pattern builds upon previous reports, such as those by Martínez-
273 Campos et al., who observed highly diverse bacterial assemblages on biodegradable MPs
274 compared to conventional ones²⁴. However, the observed trends indicate that this elevated
275 diversity on PLA may represent a transient phase during mid-stage colonization rather than a
276 permanent characteristic of the mature biofilm. Among the conventional, non-biodegradable
277 polymers, distinct patterns emerged. By day 30, diversity within the PS-associated biofilm
278 developed to be the highest across all tested MPs. In contrast, the polyolefin PP maintained the
279 lowest diversity throughout the entire 30-day incubation. Meanwhile, PE and the polyester PET
280 exhibited higher initial diversity that subsequently decreased as the plastispheres matured.
281 Ultimately, the unique diversity dynamics observed on each polymer type indicate strong
282 surface-specific selection. This is consistent with literature establishing that microplastic
283 properties, rather than simple bulk biomass, are the primary drivers of plastisphere
284 composition³².

285 Beta diversity was visualized using Principal Coordinate Analysis (PCoA) based on Bray–
286 Curtis dissimilarities (Figure 3 (2)). Across all time points at days 3, 15, and 30, the most



287 prominent trend was the distinct and consistent separation of the control sludge from the
288 microplastic-associated biofilms. The control sludge occupied an isolated position in the
289 ordination space, confirming that the microplastics did not merely recruit a random subset of
290 the surrounding microbial community. Instead, the solid polymer surfaces exerted a strong
291 selective pressure that drove the assembly of a highly specialized plastisphere, a phenomenon
292 consistent with previous studies demonstrating that microplastics host microbial assemblages
293 inherently distinct from their surrounding bulk environments²¹. Axis 1 and Axis 2 represented
294 the dominant gradients in community dissimilarity, expressed as variance explained. The
295 magnitude of this compositional divergence between the suspended sludge and the surface-
296 attached communities became more pronounced as the biofilms matured, with the variance
297 explained by the primary gradient on Axis 1 increasing from 40.4 % at day 3 to 67.0 % by day
298 30.

299 During early colonization (day 3), the ordination revealed a wide dispersion among the
300 plastispheres, driven by two primary gradients in community dissimilarity (Axis 1 = 40.4 %,
301 Axis 2 = 27.6 %) (Figure 3 (2a)). Unlike the later stages of incubation where certain
302 communities began to converge, the day 3 plastispheres were highly distinct from one another,
303 scattering widely across the ordination space. This broad distribution suggests that multiple
304 factors, such as polymer composition, surface chemistry (surface charge, hydrophobicity), and
305 physical characteristics (roughness, topography), acted synergistically during early biofilm
306 formation, rather than a single dominant property dictating the community structure. Notably,
307 PP occupied a distinct position, segregating entirely from other polyolefins like PE along the
308 primary axis. This early divergence is consistent with reports that pristine PP exhibits greater
309 surface roughness and microtopography, which can alter conditioning-film adsorption and
310 initial microbial attachment, thereby yielding divergent early community structures³³. Overall,

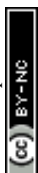


311 these distinct spatial patterns confirm that rapid, polymer-specific selective colonization occurs
312 within the first three days of exposure.

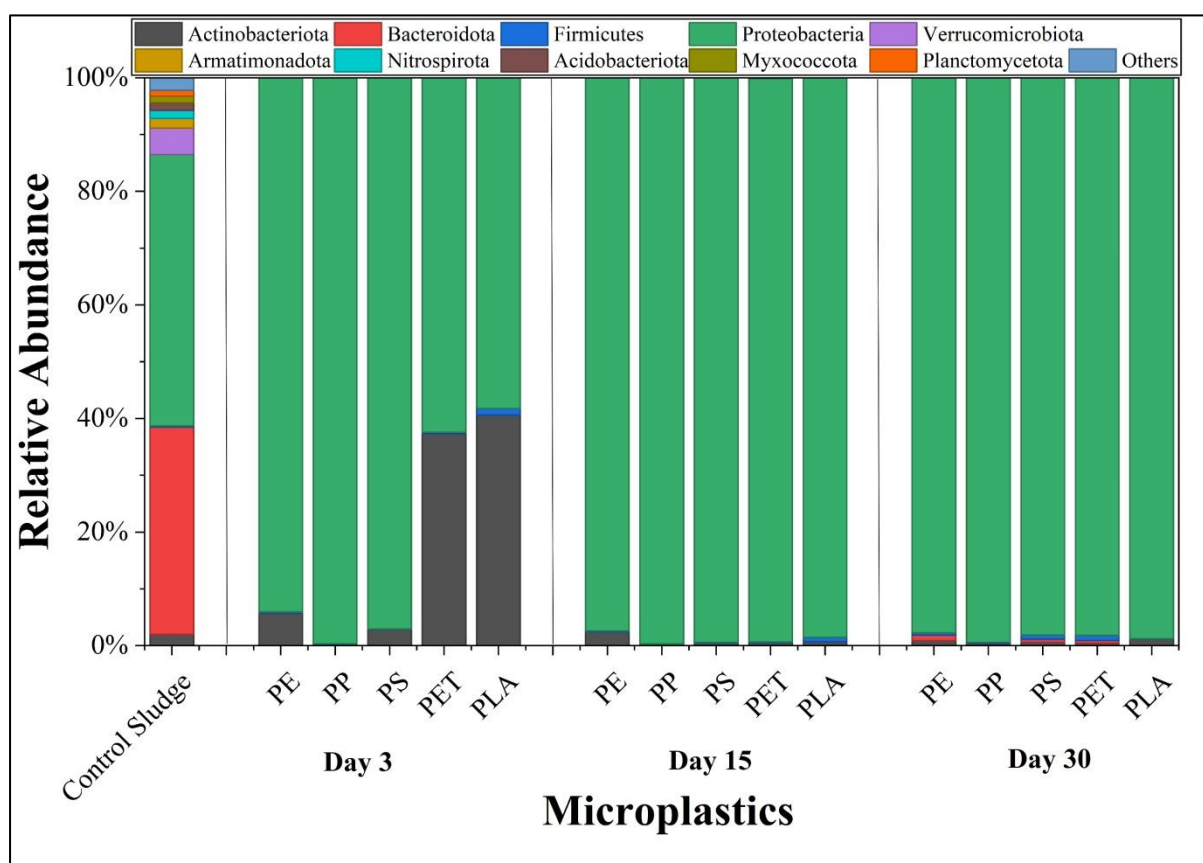
313 During the growth and maturation phase (days 15 and 30), distinct community dynamics
314 emerged within the plastsphere (Figure 3 (2b–c)). At day 15, the communities on the
315 conventional polymers began to group together, whereas the biodegradable PLA diverged
316 distinctly along Axis 2. By day 30, the community structures on PE, PP, and PET converged
317 into a highly compact cluster. This convergence suggests that the development of mature
318 biofilms and extensive surface conditioning ultimately diminished the impact of their initial
319 surface chemistry differences. In contrast, PLA and PS remained highly isolated from this
320 central polyolefin and polyester cluster by day 30, separating in opposite directions along Axis
321 2. In contrast, PLA and PS remained highly isolated from this central polyolefin and polyester
322 cluster by day 30, separating in opposite directions along Axis 2. The persistent spatial offset
323 of PLA aligns with biodegradability-driven hydrolytic aging, which alters surface polarity and
324 micro-roughness to support a distinct community. Meanwhile, the distinct trajectory of the PS
325 biofilm reflects the unique selective pressure by its higher surface energy and aromatic
326 structure. Overall, these ordination patterns evidence that while certain conventional polymers
327 host convergent communities upon maturation, distinct material properties such as
328 biodegradability or aromaticity continue to drive highly specialized selective colonization over
329 time.

330 3.2.2. Taxonomic structure and composition

331 The control sludge community was co-dominated by Proteobacteria (47.8 %) and Bacteroidota
332 (36.5 %), a profile typical of biological treatment systems. In contrast, a distinct plastsphere
333 assembled rapidly on the MPs (Figure 4). During early colonization (day 3), biofilms were
334 mainly composed of Proteobacteria together with Actinobacteriota, approaching ~99 % across



335 polymers. This represented a drastic shift from the control sludge, as Bacteroidota was nearly
 336 completely excluded from the early MP biofilms. Early polymer-specific colonization was
 337 evident: PET and PLA co-enriched Actinobacteriota to about 37–41 %, representing a massive
 338 enrichment compared to its minor presence (2 %) in the control sludge, consistent with higher
 339 diversity at this stage. Greater surface polarity, which promoted conditioning-film adsorption
 340 and cation bridging, likely contributed to these patterns. In contrast, polyolefins (PE, PP) and
 341 PS were nearly exclusively Proteobacteria, consistent with prior reports of Proteobacteria
 342 enrichment on polyolefin surfaces in MP-associated plastispheres within SBRs³³.



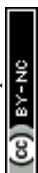
343
 344 Figure 4. Phylum-level community composition of MP-associated biofilms over time (3d,
 345 15d, and 30d).

346 Through growth and maturation (days 15 and 30), communities converged toward near-
 347 complete domination by Proteobacteria, accounting for ~99 % of all MPs. Weak but

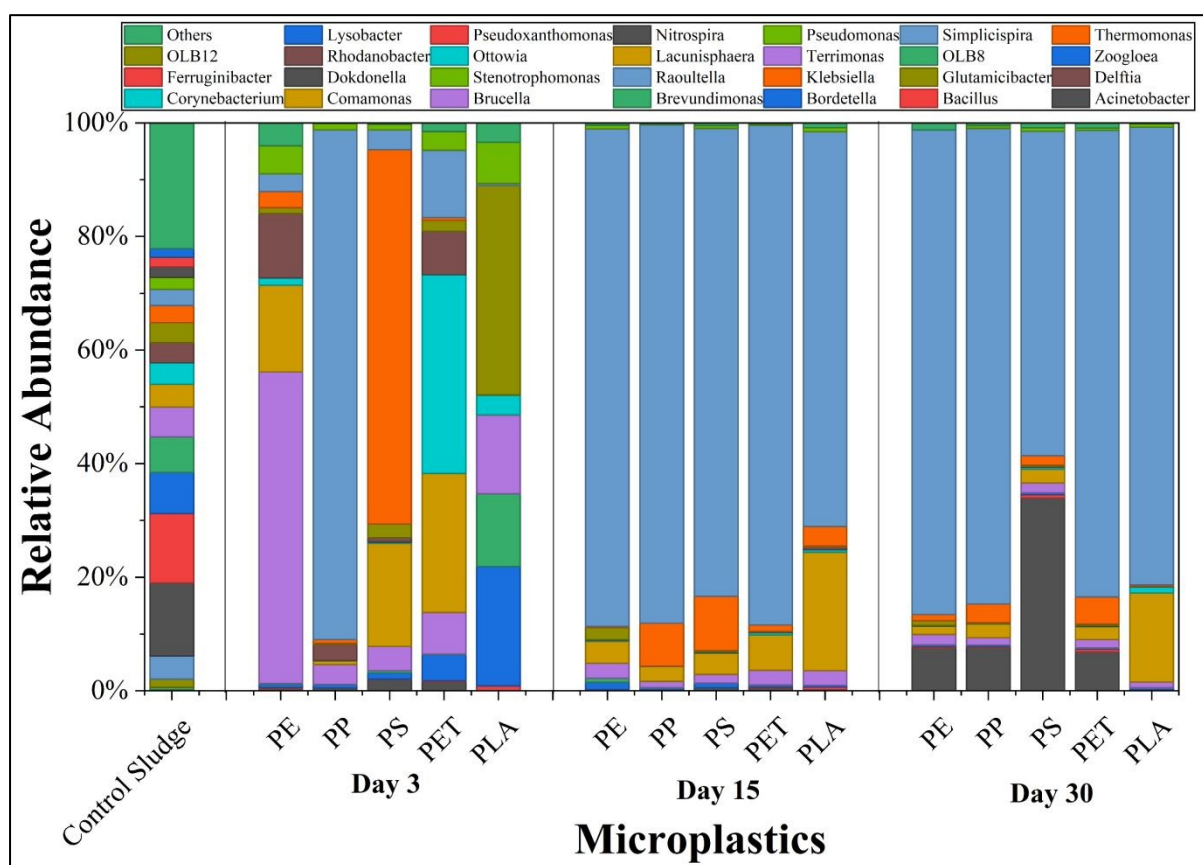


348 reproducible residues persisted, with Bacteroidota more evident on PE, and PP, Firmicutes on
349 PET, and Actinobacteriota on PLA. This rapid divergence from the planktonic baseline and the
350 consolidation toward Proteobacteria over time indicated strong surface-mediated selective
351 colonization on MPs driven by material properties such as surface energy, polarity, and
352 biodegradability. These patterns were consistent with reports that
353 Proteobacteria, Actinobacteriota, Bacteroidota, and Firmicutes were versatile biofilm formers
354 frequently enriched on MPs, including plastic-degrading and pathogenic lineages^{34–36}.
355 The distinctive bacterial compositions in the planktonic and MP-associated biofilms were more
356 revealing at the genus level. For instance, planktonic sludge communities were dominated by
357 *Dokdonella*, *Ferruginibacter*, *Zoogloea*, and the nitrifiers *Nitrosomonas* and *Nitrospira*,
358 spanning roughly 1–18 % each (Figure 5). In contrast, MP-associated biofilms displayed a
359 markedly different genus profile, emphasizing selective colonization on polymer surfaces
360 (Figure 5). MP biofilms were enriched in Enterobacterales (notably *Raoultella* and, to a lesser
361 extent, *Klebsiella*), together with Betaproteobacteria such as *Comamonas* and *Bordetella*, and
362 Actinobacteria including *Corynebacterium* and *Glutamicibacter*. This divergence from the
363 planktonic communities highlighted the plastisphere as a distinct ecological niche shaped by
364 polymer identity and exposure time.

365 During early colonization (day 3), MP type selectively enriched distinct and diverse pioneer
366 assemblages consistent with the observed diversity patterns and similar to the early
367 colonization patterns reported by Martínez-Campos et al. (2021)²⁴. Hydrophobic and aromatic
368 surfaces selected Enterobacterales-rich biofilms: PP was dominated by *Raoultella* (~90 %), a
369 prolific EPS producer and PS by *Klebsiella* (~66 %), a recognized opportunistic pathogen,
370 consistent with Kelly et al. (2021) and Bydalek et al. (2023), who identified *Klebsiella* as a key
371 pathogenic taxon enriched on MPs in wastewater systems^{37,38}. In contrast, PET and PLA
372 surfaces were dominated by Actinobacteria-linked pioneers: PET hosted *Corynebacterium*



373 (~35 %) with *Comamonas* (~25 %), and PLA enriched *Glutamicibacter* (~37 %) with
 374 *Bordetella*. This aligns with Wilkes et al. (2024) and Jiao et al. (2024), who demonstrated
 375 *Comamonas* enrichment on PET³⁷, and *Actinobacteria* dominated PLA biofilms³⁸. These
 376 dominant taxa were known early colonizers in wastewater, capable of robust biofilm formation
 377 and metabolism of organics. The pattern indicated selective colonization driven by surface
 378 chemistry.



379
 380 Figure 5. Genus-level community composition of MP-associated biofilms over time (3d, 15d,
 381 and 30d).

382 During the growth and maturation phase, by day 15, MP biofilms were dominated by
 383 *Raoultella* on all polymers (~69–88 %), with *Klebsiella* as a secondary constituent, an EPS-
 384 rich consortium that explains the decline in evenness at this stage. This functional dominance
 385 aligns with findings by Pham et al. (2021) showing *Raoultella ornithinolytica* as a significantly

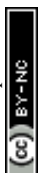


386 enriched taxon on MPs with 1.6–3.3 enrichment indices⁴¹. Although distinct polymer signals
387 persisted: on PLA, *Comamonas* comprised ~21 %; on PS, *Klebsiella* remained at ~9–10 %; on
388 PET, minor *Actinobacteria* persisted.

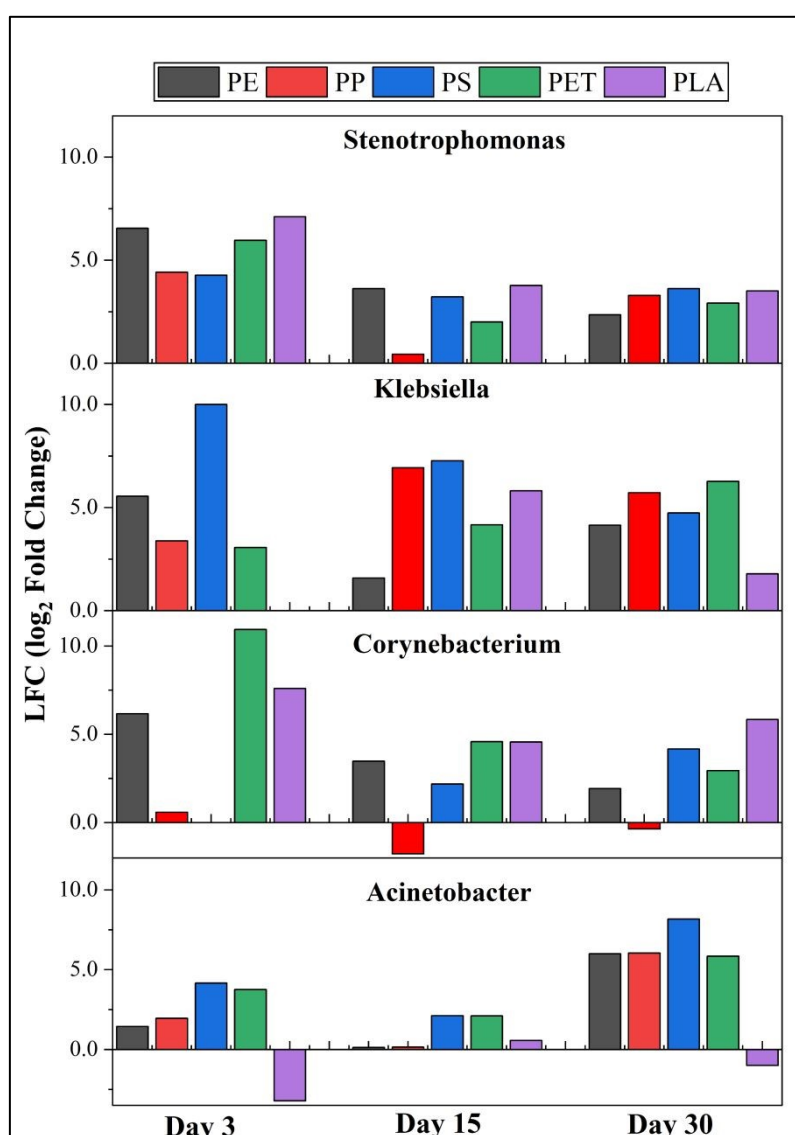
389 By day 30, convergence remained, but polymer-linked features sharpened. *Raoultella*
390 accounted for ~82–86 % on PE, PP, PET, and PLA, accompanied by *Acinetobacter* at ~6–8 %.
391 PS showed the largest shift, with *Acinetobacter* rising to ~34 % and co-dominating with
392 *Raoultella*. Kim et al. (2025) also demonstrated that *Acinetobacter sp.* exhibits dose-dependent
393 higher EPS production and enhanced biofilm formation on PS MPs⁴². PLA continued to show
394 greater representation of *Comamonas* (~16 %) than other MPs, supporting findings that
395 biodegradable polymer biofilms retain distinct bacterial compositions with degradative
396 capabilities. Functionally, these profiles indicated enrichment of opportunistic pathogen–
397 associated genera on some materials by late maturation, particularly PS with high
398 *Acinetobacter* and sustained Enterobacterales, whereas PLA supported a higher fraction of
399 degraders such as *Comamonas*. This pattern supported surface-driven selection followed by
400 functional convergence on EPS-producing Enterobacterales, with partial diversification at day
401 30 and persistent polymer-specific signatures in the mature plastisphere. This temporal
402 succession pattern mirrors Tagg et al. (2022) findings showing polymer type shapes biofilm
403 maturation and pathogen dynamics over extended incubation periods⁴³.

404 3.2.3. Pathogen enrichment in MP-associated biofilms

405 MP-associated biofilms contained higher proportions of risk-relevant taxa than the control
406 sludge, including groups of clinical and veterinary concern. This enrichment was quantified
407 using log₂-fold-change (LFC), which measures the binary logarithm of the ratio between
408 biofilm and control sludge relative abundances, with positive values indicating enrichment in
409 MP-associated biofilms⁴⁴. Among the dominant genera detected on MPs (Figure 6),



410 *Acinetobacter* and *Klebsiella*, members of the ESKAPE pathogens, exhibited substantial
 411 enrichment in the plastisphere, with maximum LFCs of 8.17 and 10.01, respectively. This
 412 reflects their well-known capacities for biofilm formation and antimicrobial resistance⁴⁵.
 413 *Stenotrophomonas* and some *Corynebacterium*, recognized opportunistic pathogens in
 414 biological wastewater treatment systems that have also been implicated in fish disease in
 415 aquaculture settings⁴⁶, showed maximum LFCs of 7.11 and 10.93, respectively, indicating their
 416 selective enrichment within MP biofilms.



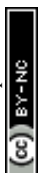
417



418 Figure 6. Differential enrichment, expressed as log₂ fold change (LFC), of genera comprising
419 key pathogenic species observed in microplastic-associated biofilms at different incubation
420 times (days 3, 15, and 30).

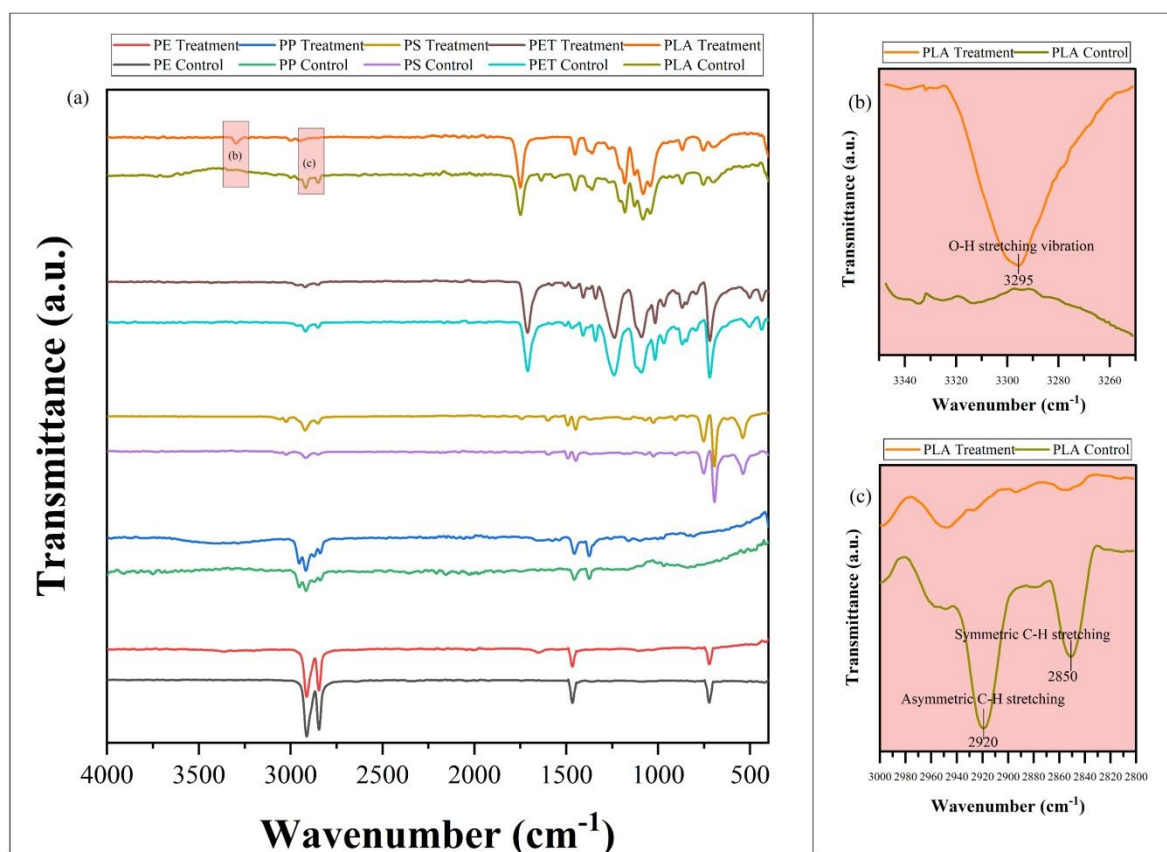
421 Across time, pathogen-associated genera on MPs exhibited polymer-specific succession
422 (Figure 6). During early colonization (day 3), *Klebsiella* was heavily enriched on PS, showing
423 a maximum LFC of 10.01, while PET strongly selected for *Corynebacterium*, reaching an LFC
424 of 10.93. By day 15, the enrichment of *Klebsiella* declined on PS but increased on PET and PP
425 to LFCs of 4.16 and 6.93, respectively, indicating material-specific selection during the biofilm
426 growth phase. By day 30, *Acinetobacter* proliferated across all non-biodegradable conventional
427 polymers, reaching LFCs between 5.85 and 8.17, with the highest enrichment observed on PS.
428 Meanwhile, the initial strong enrichment of pioneer colonizers such as *Stenotrophomonas* and
429 *Corynebacterium* generally contracted across most materials as the biofilms matured.
430 Additionally, Members of *Nocardiaceae*, frequently observed in treatment plants and including
431 clinically significant *Nocardia* spp., were also enriched in MP biofilms⁴⁷ (Supporting
432 Information, Figure S1). These observations indicated that the platisphere can act as a
433 selective substrate for pathogen-associated lineages relative to the surrounding sludge⁴⁸.

434 Taken together, the genus-level data showed polymer-dependent succession that concentrated
435 opportunistic pathogens on specific MPs. PS carried consistently high burdens of these taxa
436 throughout the maturation phase, whereas the biodegradable PLA exhibited the lowest overall
437 enrichment by day 30. These taxa are likely embedded in EPS-rich matrices that promote
438 adhesion, protect against oxidants, and concentrate extracellular DNA, thereby supporting
439 persistence through biological treatment systems. Consequently, platisphere-associated
440 pathogens on selected polymers may be exported in effluents or sludges despite overall
441 treatment reduction, posing risks to aquatic organisms and human health⁹.



442 3.3. Physicochemical properties of MPs post-exposure

443 The selective enrichment of specific bacterial genera, including pathogens, capable of MP
 444 degradation in WWTPs, led to measurable property changes after 30 days in SBRs. PLA MPs
 445 exhibited clear signs of degradation, evidenced by distinct spectral alterations in the ATR-FTIR
 446 analysis, whereas PE, PP, PS, and PET remained largely stable (Figure 7 (a)).



447
 448 Figure 7. Physicochemical changes of microplastics after 30 days in SBRs: ATR-FTIR
 449 spectra for PE, PP, PS, PET, and PLA before (control) and after exposure (treatment).

450 The PLA spectra, as shown in Figure 7(b), displayed a significant increase in the broad
 451 absorption band at 3295 cm⁻¹, which is characteristic of the O-H stretching vibration of
 452 hydroxyl end groups. This change strongly indicates the occurrence of hydrolytic chain scission
 453 of the ester bonds. Concurrently, the intensity of the characteristic aliphatic C-H stretching
 454 peaks at 2920 cm⁻¹ (asymmetric C-H) and 2850 cm⁻¹ (symmetric C-H) was reduced (Figure

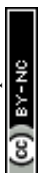


455 7(c)), reflecting the surface degradation and subsequent microbial uptake of the resulting short-
456 chain molecules. Furthermore, the modest increases in carbonyl and C–O stretching bands
457 between 1760 and 1080 cm^{-1} confirm the formation of other polar degradation products (such
458 as carboxylic acid end groups), which collectively enhance the PLA surface wettability and
459 correlate with the greater biomass accumulation observed on PLA MPs⁴⁹.

460 Morphological analysis via SEM further corroborated the chemical changes, showing that PLA
461 exhibited localized pitting, fissures, and etched domains, consistent with active microbial or
462 enzymatic attack on the polymer matrix (Supporting Information, Figure S2). In contrast, the
463 PS MPs primarily displayed edge chipping, abrasion tracks, and minor surface scuffs, features
464 characteristic of mechanical wear from mixing and shear against the reactor walls⁵⁰. The lack
465 of significant chemical change in conventional MPs indicated their resistance to substantial
466 biofilm-mediated oxidation under the short-term SBR conditions. The distinct PLA
467 morphology aligns with its surface oxidation and increased micro-roughness, which enhance
468 wettability and provide additional anchoring sites for EPS. PS, meanwhile, developed
469 microstructures that improve physical retention but lack clear FTIR-detectable oxidation.
470 Together, the spectroscopic and microscopic evidence demonstrate polymer-specific
471 weathering pathways over 30 days: PLA undergoes measurable chemical modification driven
472 by microbial activity, whereas PS experiences predominantly mechanical alteration.

473 **Conclusion**

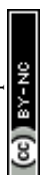
474 This study demonstrates that biofilm formation on MPs within biological wastewater treatment
475 units is strongly governed by polymer-specific surface properties and biodegradability,
476 resulting in distinct patterns of biomass accumulation and microbial community composition.
477 Biofilm development followed material-dependent colonization trajectories, with
478 biodegradable PLA consistently supporting the highest biofilm biomass. While PLA promoted



479 a transient peak in microbial diversity and the selective enrichment of plastic-degrading taxa,
480 such as *Comamonas*, coincided with pronounced hydrolytic aging and surface pitting,
481 indicating that polymer degradability plays an important role in shaping later-stage plastisphere
482 succession. Although, these dynamic surface alterations did not favour the long-term retention
483 of opportunistic pathogens. In contrast, log₂-fold-change analysis revealed that highly stable
484 conventional MPs, particularly PS, supported the highest and most persistent enrichment of
485 specific risk-relevant taxa, including *Acinetobacter* and *Klebsiella*, by the mature biofilm stage.
486 This distinction suggests that while biodegradable surfaces promote robust general microbial
487 growth, the structural permanence of conventional polymers provides a more selective and
488 reliable substrate for pathogen persistence within WWTPs.

489 Collectively, these findings reveal the plastisphere as a critical biological interface mediating
490 MP–microbe interactions in wastewater treatment systems. While biofilm-associated processes
491 may contribute to polymer surface modification and weathering, the extent to which such
492 processes lead to fragmentation into nano plastics, and how intermediate degradation products
493 (such as oligomers and monomers) from biodegradable polymers impact overall microbial
494 health, remains unresolved. Future research should therefore prioritize long-term, multi-year
495 in situ studies incorporating mixed polymer profiles to evaluate their combined impacts on
496 sludge settling and the safety of final agricultural sludge reuse. Additionally, while pathogen
497 retention was clearly demonstrated, the relative risk of antibiotic resistance gene (ARG)
498 proliferation and spread via biodegradable versus conventional biofilms requires targeted,
499 standardized investigation. Recognizing the dual role of MP-associated biofilms in both
500 pathogen retention and polymer transformation is essential for developing a comprehensive
501 understanding of microplastic fate and behaviour within WWTPs.

502 **Acknowledgment**



503 This research was funded by the Natural Sciences and Engineering Research Council
504 (Discovery Grant 23451, NSERC Alliance Option-2 Grants, ALLRP 571066 - 21),
505 "Microplastics in Sewage Sludge Exploration and Detection (MISSED)" project. We would
506 also like to thank James and Joanne Love, Chair in Environmental Engineering, for their
507 financial support. The authors gratefully acknowledge Ripley's Aquarium for their knowledge
508 mobilization efforts, the Surette Lab and the McMaster Genomics Facility for their sequencing
509 assistance, and Dr. Magdalena Jaklewicz at the York University Imaging Facility for her
510 valuable help with the SEM analysis.

511 **Author contributions: CRediT:** Gaurav Bhardwaj: Conceptualization, Methodology,
512 Investigation, Validation, Formal analysis, Writing – original draft, Writing – review & editing.
513 Lachi Wankhede: Methodology, Writing – review & editing. Ratul Kumar Das: Writing –
514 review & editing. Ahmed ElDyasti: Supervision, Writing – review & editing. Ahmed Koubaa:
515 Supervision, Writing – review & editing. Satinder Brar: Supervision, Funding acquisition,
516 Writing – review & editing.

517 **Data availability:** The sequence data generated and analyzed during the current study has been
518 deposited in the Sequence Read Archive (SRA) maintained by the National centre for
519 Biotechnology Information (NCBI) under the Bio Project ID PRJNA1436619 (Title: Microbial
520 diversity in MP-associated biofilms in WWTPs). All other data supporting the findings of this
521 study are available within the article and its corresponding supporting information file.

522 References

- 523 1 L. K. DH, G. Bhardwaj, R. Indhur, L. Wankhede, S. K. Brar and S. Kumari,
524 Electrochemical approaches for detecting micro and nano-plastics in different
525 environmental matrices, *International Journal of Electrochemical Science*, 2025, **20**,
526 101182.
- 527 2 J. Li, H. Liu and J. Paul Chen, Microplastics in freshwater systems: A review on
528 occurrence, environmental effects, and methods for microplastics detection, *Water*
529 *Research*, 2018, **137**, 362–374.



- 530 3 E. R. Zettler, T. J. Mincer and L. A. Amaral-Zettler, Life in the “plastisphere”: microbial
531 communities on plastic marine debris, *Environ Sci Technol*.
- 532 4 H.-C. Flemming and J. Wingender, The biofilm matrix, *Nat Rev Microbiol*, 2010, **8**, 623–
533 633.
- 534 5 M. Arias-Andres, U. Klümper, K. Rojas-Jimenez and H.-P. Grossart, Microplastic
535 pollution increases gene exchange in aquatic ecosystems, *Environmental Pollution*, 2018,
536 **237**, 253–261.
- 537 6 J. S. Madsen, M. Burmølle, L. H. Hansen and S. J. Sørensen, The interconnection between
538 biofilm formation and horizontal gene transfer, *FEMS Immunol Med Microbiol*, 2012, **65**,
539 183–195.
- 540 7 G. Bhardwaj, M. Abdulkadhim, K. Joshi, L. Wankhede, R. K. Das and S. K. Brar,
541 Exposure Pathways, Systemic Distribution, and Health Implications of Micro- and
542 Nanoplastics in Humans, *Applied Sciences*, 2025, **15**, 8813.
- 543 8 X. Wu, J. Pan, M. Li, Y. Li, M. Bartlam and Y. Wang, Selective enrichment of bacterial
544 pathogens by microplastic biofilm, *Water Research*, 2019, **165**, 114979.
- 545 9 G. Bhardwaj, L. Wankhede, R. Pulicharla and S. K. Brar, Microplastic-associated
546 biofilms in wastewater treatment plants: Mechanisms and impacts, *Journal of Water
547 Process Engineering*, 2025, **72**, 107582.
- 548 10 S. Oberbeckmann, B. Kreikemeyer and M. Labrenz, Environmental Factors Support the
549 Formation of Specific Bacterial Assemblages on Microplastics, *Front Microbiol*, 2017,
550 **8**, 2709.
- 551 11 K. Parrish and N. L. Fahrenfeld, Microplastic biofilm in fresh- and wastewater as a
552 function of microparticle type and size class, *Environ. Sci.: Water Res. Technol.*, 2019, **5**,
553 495–505.
- 554 12 S. Rajcoomar, I. D. Amoah, T. Abunama, N. Mohlomi, F. Bux and S. Kumari, Biofilm
555 formation on microplastics in wastewater: insights into factors, diversity and inactivation
556 strategies, *Int. J. Environ. Sci. Technol.*, DOI:10.1007/s13762-023-05266-0.
- 557 13 G. Bhardwaj, M. Mohammadiun, C. S. Osorio Gonzalez, S. Kaur Brar and S. Karimpour,
558 Wastewater-induced microplastic biofouling in freshwater: role of particle size and flow
559 velocity, *Environ. Sci.: Adv.*, DOI:10.1039/D4VA00303A.
- 560 14 M. Zarean, S. H. Dave, S. K. Brar and R. W. M. Kwong, Environmental drivers of
561 antibiotic resistance: Synergistic effects of climate change, co-pollutants, and
562 microplastics, *Journal of Hazardous Materials Advances*, 2025, **19**, 100768.
- 563 15 C. Li, L. Wang, S. Ji, M. Chang, L. Wang, Y. Gan and J. Liu, The ecology of the
564 plastisphere: Microbial composition, function, assembly, and network in the freshwater
565 and seawater ecosystems, *Water Research*, 2021, **202**, 117428.
- 566 16 S. Oberbeckmann and M. Labrenz, Marine Microbial Assemblages on Microplastics:
567 Diversity, Adaptation, and Role in Degradation, *Ann Rev Mar Sci*, 2020, **12**, 209–232.
- 568 17 F. Murphy, C. Ewins, F. Carbonnier and B. Quinn, Wastewater Treatment Works
569 (WwTW) as a Source of Microplastics in the Aquatic Environment, *Environ Sci Technol*,
570 2016, **50**, 5800–5808.
- 571 18 X. Li, L. Chen, Q. Mei, B. Dong, X. Dai, G. Ding and E. Y. Zeng, Microplastics in sewage
572 sludge from the wastewater treatment plants in China, *Water Research*, 2018, **142**, 75–
573 85.
- 574 19 S. Huang, B. Zhang, Z. Zhao, C. Yang, B. Zhang, F. Cui, P. N. L. Lens and W. Shi,
575 Metagenomic analysis reveals the responses of microbial communities and nitrogen
576 metabolic pathways to polystyrene micro(nano)plastics in activated sludge systems,
577 *Water Research*, 2023, **241**, 120161.



- 578 20 B. Zhang, S. Huang, L. Wu, Y. Guo, W. Shi and P. N. L. Lens, Micro(nano)plastic size
579 and concentration co-differentiate the treatment performance and toxicity mechanism in
580 aerobic granular sludge systems, *Chemical Engineering Journal*, 2023, **457**, 141212.
- 581 21 Q. Li, L. Tian, X. Cai, Y. Wang and Y. Mao, Plastisphere showing unique microbiome
582 and resistome different from activated sludge, *Science of The Total Environment*, 2022,
583 **851**, 158330.
- 584 22 Y. Feng, J.-W. Sun, W.-W. Shi, J.-L. Duan, X.-D. Sun, L.-J. Feng, Q. Wang, Y.-D. Gan
585 and X.-Z. Yuan, Microplastics exhibit accumulation and horizontal transfer of antibiotic
586 resistance genes, *Journal of Environmental Management*, 2023, **336**, 117632.
- 587 23 L. Shen, Y. Wang, R. Liu, Y. Yang, Y. Liu and B. Xing, Aging characteristics of
588 degradable and non-biodegradable microplastics and their adsorption mechanism for
589 sulfonamides, *Science of The Total Environment*, 2023, **901**, 166452.
- 590 24 S. Martínez-Campos, M. González-Pleiter, F. Fernández-Piñas, R. Rosal and F. Leganés,
591 Early and differential bacterial colonization on microplastics deployed into the effluents
592 of wastewater treatment plants, *Science of The Total Environment*, 2021, **757**, 143832.
- 593 25 G. Bhardwaj, R. K. Das, A. Eldyasti, A. Koubaa and S. K. Brar, Differential impacts of
594 conventional and biodegradable microplastics on treatment performance and bacterial
595 community in sequencing batch reactors, *Bioresource Technology Reports*, 2025, **32**,
596 102344.
- 597 26 K. Yang, Q.-L. Chen, M.-L. Chen, H.-Z. Li, H. Liao, Q. Pu, Y.-G. Zhu and L. Cui,
598 Temporal Dynamics of Antibiotic Resistome in the Plastisphere during Microbial
599 Colonization, *Environ. Sci. Technol.*, 2020, **54**, 11322–11332.
- 600 27 D. Lobelle and M. Cunliffe, Early microbial biofilm formation on marine plastic debris,
601 *Mar Pollut Bull*.
- 602 28 B. J. Callahan, P. J. McMurdie, M. J. Rosen, A. W. Han, A. J. A. Johnson and S. P.
603 Holmes, DADA2: High-resolution sample inference from Illumina amplicon data, *Nat*
604 *Methods*, 2016, **13**, 581–583.
- 605 29 Y. Lu, G. Zhou, J. Ewald, Z. Pang, T. Shiri and J. Xia, MicrobiomeAnalyst 2.0:
606 comprehensive statistical, functional and integrative analysis of microbiome data, *Nucleic*
607 *Acids Res*, 2023, **51**, W310–W318.
- 608 30 Y. Wang, X. Liu, C. Huang, W. Han, P. Gu, R. Jing and Q. Yang, Antibiotic resistance
609 genes and virulence factors in the plastisphere in wastewater treatment plant effluent:
610 Health risk quantification and driving mechanism interpretation, *Water Research*, 2025,
611 **271**, 122896.
- 612 31 K. P. Lai, C. F. Tsang, L. Li, R. M. K. Yu and R. Y. C. Kong, Microplastics act as a
613 carrier for wastewater-borne pathogenic bacteria in sewage, *Chemosphere*, 2022, **301**,
614 134692.
- 615 32 M. Ogonowski, A. Motiei, K. Ininbergs, E. Hell, Z. Gerdes, K. I. Udekwa, Z. Bacsik and
616 E. Gorokhova, Evidence for selective bacterial community structuring on microplastics,
617 *Environmental Microbiology*, 2018, **20**, 2796–2808.
- 618 33 D. K. Tuyen, S. Jeong, K. Cho and H.-T. Nguyen, Biological treatment shaping
619 microplastic-associated microbial communities in wastewater treatment plant, *Journal of*
620 *Water Process Engineering*, 2025, **76**, 108120.
- 621 34 X. Guo, Y.-R. Chen, X. Sun, C. Li, L. Hou, M. Liu and Y. Yang, Plastic properties affect
622 the composition of prokaryotic and eukaryotic communities and further regulate the
623 ARGs in their surface biofilms, *Science of The Total Environment*, 2022, **839**, 156362.
- 624 35 J.-W. Lee, J.-H. Nam, Y.-H. Kim, K.-H. Lee and D.-H. Lee, Bacterial communities in the
625 initial stage of marine biofilm formation on artificial surfaces, *J Microbiol.*, 2008, **46**,
626 174–182.



- 627 36 L. Miao, P. Wang, J. Hou, Y. Yao, Z. Liu, S. Liu and T. Li, Distinct community structure
628 and microbial functions of biofilms colonizing microplastics, *Science of The Total*
629 *Environment*, 2019, **650**, 2395–2402. View Article Online
DOI: 10.1039/C9VA00023A
- 630 37 J. J. Kelly, M. G. London, A. R. McCormick, M. Rojas, J. W. Scott and T. J. Hoellein,
631 Wastewater treatment alters microbial colonization of microplastics, *PLoS ONE*,
632 DOI:10.1371/journal.pone.0244443.
- 633 38 F. Bydalek, G. Webster, R. Barden, A. J. Weightman, B. Kasprzyk-Hordern and J. Wenk,
634 Microplastic biofilm, associated pathogen and antimicrobial resistance dynamics through
635 a wastewater treatment process incorporating a constructed wetland, *Water Research*,
636 DOI:10.1016/j.watres.2023.119936.
- 637 39 R. A. Wilkes, N. Zhou, A. L. Carroll, O. Aryal, K. P. Teitel, R. S. Wilson, L. Zhang, A.
638 Kapoor, E. Castaneda, A. M. Guss, J. R. Waldbauer and L. Aristilde, Mechanisms of
639 Polyethylene Terephthalate Pellet Fragmentation into Nanoplastics and Assimilable
640 Carbons by Wastewater Comamonas, *Environ. Sci. Technol.*, 2024, **58**, 19338–19352.
- 641 40 Y. Jiao, A. Zhou, D. Zhang, M. Chen and L. Wan, Distinct microbial community
642 structures formed on the biofilms of PLA and PP, influenced by physicochemical factors
643 of sediment and polymer types in a 60-day indoor study, *Front. Environ. Sci.*,
644 DOI:10.3389/fenvs.2024.1452523.
- 645 41 D. N. Pham, L. Clark and M. Li, Microplastics as hubs enriching antibiotic-resistant
646 bacteria and pathogens in municipal activated sludge, *Journal of Hazardous Materials*
647 *Letters*, 2021, **2**, 100014.
- 648 42 S. Y. Kim, S. Woo, S.-W. Lee, E.-M. Jung and E.-H. Lee, Dose-Dependent Responses of
649 Escherichia coli and Acinetobacter sp. to Micron-Sized Polystyrene Microplastics, 2025,
650 **35**, 1–10.
- 651 43 A. S. Tagg, T. Sperlea, M. Labrenz, J. P. Harrison, J. J. Ojeda and M. Sapp, Year-Long
652 Microbial Succession on Microplastics in Wastewater: Chaotic Dynamics Outweigh
653 Preferential Growth, *Microorganisms*, 2022, **10**, 1775.
- 654 44 M. I. Love, W. Huber and S. Anders, Moderated estimation of fold change and dispersion
655 for RNA-seq data with DESeq2, *Genome Biology*, 2014, **15**, 550.
- 656 45 D. M. P. De Oliveira, B. M. Forde, T. J. Kidd, P. N. A. Harris, M. A. Schembri, S. A.
657 Beatson, D. L. Paterson and M. J. Walker, Antimicrobial Resistance in ESKAPE
658 Pathogens, *Clinical Microbiology Reviews*, 2020, **33**, 10.1128/cmr.00181-19.
- 659 46 A. Pękala-Safińska, Contemporary threats of bacterial infections in freshwater fish,
660 *Journal of Veterinary Research*, 2018, **62**, 261–267.
- 661 47 S. Jia and X. Zhang, in *High-Risk Pollutants in Wastewater*, eds H. Ren and X. Zhang,
662 Elsevier, 2020, pp. 41–78.
- 663 48 M. Shen, Z. Zeng, L. Li, B. Song, C. Zhou, G. Zeng, Y. Zhang and R. Xiao, Microplastics
664 act as an important protective umbrella for bacteria during water/wastewater disinfection,
665 *Journal of Cleaner Production*, 2021, **315**, 128188.
- 666 49 J. Brandon, M. Goldstein and M. D. Ohman, Long-term aging and degradation of
667 microplastic particles: Comparing in situ oceanic and experimental weathering patterns,
668 *Marine Pollution Bulletin*, 2016, **110**, 299–308.
- 669 50 S. Monira, R. Roychand, F. I. Hai, M. Bhuiyan and B. K. Pramanik, Microplastic
670 fragmentation into nanoplastics by water shear forces during wastewater treatment:
671 Mechanical insights and theoretical analysis, *Environmental Pollution*, 2025, **364**,
672 125310.
673



Data availability statement

View Article Online
DOI: 10.1039/D6VA00023A

The sequence data generated and analyzed during the current study has been deposited in the Sequence Read Archive (SRA) maintained by the National centre for Biotechnology Information (NCBI) under the Bio Project ID PRJNA1436619 (Title: Microbial diversity in MP-associated biofilms in WWTPs). All other data supporting the findings of this study are available within the article and its corresponding supporting information file.

